© The American Society of Gene & Cell Therapy

Cardiac AAV9 Gene Delivery Strategies in Adult Canines: Assessment by Long-term Serial SPECT Imaging of Sodium Iodide Symporter Expression

Gilles Moulay[1], Tomohito Ohtani[2], Ozgur Ogut[1], Adam Guenzel[1], Atta Behfar[1], Rosita Zakeri[1], Philip Haines[3], Jimmy Storlie[1], Lorna Bowen[1], Linh Pham[1], David Kaye[4], Gurpreet Sandhu[1], Michael O'Connor[1], Stephen Russell[1] and Margaret Redfield[1]

[1]Mayo Clinic, Rochester, Minnesota, USA; [2]Osaka University, Osaka, Japan; [3]University of Pennsylvania, Philadelphia, Pennsylvania, USA; [4]Baker Heart Research Institute, Melbourne, Australia

Heart failure is a leading cause of morbidity and mortality, and cardiac gene delivery has the potential to provide novel therapeutic approaches. Adeno-associated virus serotype 9 (AAV9) transduces the rodent heart efficiently, but cardiotropism, immune tolerance, and optimal delivery strategies in large animals are unclear. In this study, an AAV9 vector encoding canine sodium iodide symporter (NIS) was administered to adult immunocompetent dogs via epicardial injection, coronary infusion without and with cardiac recirculation, or endocardial injection via a novel catheter with curved needle and both end- and side-holes. As NIS mediates cellular uptake of clinical radioisotopes, expression was tracked by single-photon emission computerized tomography (SPECT) imaging in addition to Western blot and immunohistochemistry. Direct epicardial or endocardial injection resulted in strong cardiac expression, whereas expression after intracoronary infusion or cardiac recirculation was undetectable. A threshold myocardial injection dose that provides robust nonimmunogenic expression was identified. The extent of transmural myocardial expression was greater with the novel catheter versus straight end-hole needle delivery. Furthermore, the authors demonstrate that cardiac NIS reporter gene expression and duration can be quantified using serial noninvasive SPECT imaging up to 1 year after vector administration. These data are relevant to efforts to develop cardiac gene delivery as heart failure therapy.

Received 19 November 2014; accepted 18 April 2015; advance online publication 2 June 2015. doi:10.1038/mt.2015.78

INTRODUCTION

Currently, the treatment of heart failure (HF) relies on several noncurative and often highly invasive strategies that are not universally available or effective. Cardiac restricted gene delivery to restore or enhance expression of proteins that have salubrious effects on cardiac function but are absent or depleted because of genetic mutations or acquired down-regulation represents a novel therapeutic approach for HF.[1] Adeno-associated virus (AAV) infection is nonpathogenic and does not require an actively dividing host cell, thus making it suitable for cardiomyocyte gene therapy. Promising initial studies in rodent HF models triggered a small number of large mammal studies[2–4] and a single human HF clinical trial was completed using AAV1 gene delivery of the sarcoplasmic reticulum Ca^{2+}-ATPase (SERCA2a)[5] via coronary infusion. The small number of patients studied and constraints on quantitation of changes in SERCA2a cardiac expression limited the ability to definitively demonstrate dose response or degree of cardiac transduction. Further preclinical studies are required to overcome various obstacles including optimal delivery strategies, dose response, and potential for immune response against the vector or transgenic protein in large animal and human heart.

The canine sodium iodide symporter (cNIS) gene is an integral membrane glycoprotein mediating cellular uptake and concentration of sodium and iodide. NIS is primarily expressed in the stomach and thyroid and is absent from the heart.[6] Standard radioisotopes used for investigational or clinical cardiac imaging (^{125}I or technetium 99m (Tc-99m)[7]) can be used to detect NIS activity using single-photon emission computerized tomography (SPECT).

The objective of this study was to evaluate cardiac transduction efficiency as assessed by serial quantitative SPECT imaging *in vivo* as well as Western blot and immunohistochemical analyses in harvested tissue following delivery of AAV9 canine NIS (AAV9-cNIS) to adult immunocompetent AAV9 seronegative canines. Several clinically relevant delivery methods were tested, including direct epicardial injection via end-hole only straight needle, intracoronary infusion without or with cardiac recirculation, and percutaneous endocardial delivery using a novel endocardial delivery catheter with a curved end- and side-hole needle (C-Cath).

The authors report that (i) direct myocardial injection (epicardial or endocardial) provides efficient cardiac transduction, whereas expression was not detectable after intracoronary infusion without or with cardiac recirculation; (ii) myocardial injection of vector doses $\leq 3 \times 10^{11}$ viral genomes (vg) per

Correspondence: Margaret Redfield, Mayo Clinic Cardiorenal Laboratory, 200 First St SW, Rochester, MN 55905, USA.
E-mail: redfield.margaret@mayo.edu

© The American Society of Gene & Cell Therapy

injection avoided cytotoxic responses with expression for up to 12 months; (iii) the extent of transmural myocardial expression following myocardial vector injection is greater with the C-Cath delivery catheter when compared with an end-hole straight needle injection; and (iv) cardiac NIS reporter gene expression and duration can be quantified using serial noninvasive SPECT imaging. These data are highly relevant to efforts to develop cardiac gene delivery for HF therapy.

RESULTS

Neutralizing antibody screening

All dogs receiving AAV9-cNIS were screened for serotype 9 capsid seropositivity using an *in vivo* neutralization assay based on the concept that passive immunization with plasma from seropositive dogs would suppress expression of an AAV9-reporter gene (human carcinoembryonic antigen (hCEA)) after subsequent intravenous (IV) vector administration to immunodeficient mice. Canine plasma induced minimal attenuation of hCEA expression (mean 11%, SD 15%, range 0–37%, $n = 13$) suggesting absence or low levels of neutralizing antibodies (**Table 1**) in agreement with earlier studies demonstrating that canine AAV9 seropositivity is rare.[8] The assay was further validated using passive immunization with plasma from dog 4 obtained 14 weeks post-AAV9-cNIS injection, resulting in 92% hCEA expression inhibition. Once relative AAV9 seronegativity was confirmed, the dogs underwent one of four AAV9-cNIS administration strategies as summarized in **Table 1**.

Table 1 Protocol summary

			AAV vector			Neutralization assay
Dog	Procedure (administration, route)		Injections	Total dose (vg)	Local dose (vg/injectate)	% transduction inhibition
1	Epicardial injection		10×0.1 ml	PBS	/	0
2				5×10^{11}	5×10^{10}	0
3				3×10^{12}	3×10^{11}	0
4				1×10^{13}	1×10^{12}	0
5	Intracoronary infusion	LAD + LCx	1×10 ml	1×10^{13}	1×10^{13}	20
6		LAD + LCx				1
7	Coronary recirculation	LCx	1×10 ml	5×10^{12}	5×10^{12}	33
8		LCx		1×10^{13}	1×10^{13}	0
9		LAD		2×10^{13}	2×10^{13}	0
10	Catheter endocardial injection		35×0.1 ml	PBS + contrast	/	31
11				1×10^{13}	2.86×10^{11}	3
12						20
13						37

	SPECT-CT imaging (time post-AAV administration)							
Dog	2 Weeks	3 Weeks	1 Month	2 Months	3 Months	6 Months	10 Months	12 Months
1	X							
2	X		X					
3	X		X		X	X	X	
4	X		X		X	X		
5	X		X		X			
6	X		X		X			
7	X		X					
8	X		X					
9	X			X				
10								
11		X			X	X		X
12		X			X	X		
13			X		X			

Dog identifier number, administration route, injectate number and volume, AAV9-cNIS dose (total and per injection), and pre-existing neutralizing antibody assessment are reported in the upper section. The lower section indicates the SPECT imaging dates after AAV administrations, each represented by a X character over gray background. Sacrifice was performed ~1 week following the last imaging point; black boxes are shown after that date.
AAV, adeno-associated virus; cNIS, canine sodium iodide symporter; LAD, left anterior descending artery; LCx, left circumflex coronary artery; PBS, phosphate buffered saline; SPECT, single-photon emission computerized tomography; vg, viral genomes.

© The American Society of Gene & Cell Therapy

Epicardial AAV9-cNIS administration

As direct epicardial injection has been successfully used to deliver an AAV9 packaged gene therapeutic in the canine,[4] the authors utilized a similar technique (**Figure 1**) to establish our ability to demonstrate dose-related cNIS cardiac expression *in vivo* over time using serial SPECT imaging. Sham injection (phosphate buffered saline (PBS)) and three escalating doses of AAV9-cNIS (split into 10 injection sites, see **Supplementary Figure S1a**) were administered (**Table 1**). In normals, Tc-99m radioisotope uptake because of endogenous NIS activity is expected in the thyroid, salivary glands, and stomach, as well as bladder radioactivity because of renal Tc-99m excretion.[9] This was evident at SPECT performed 2 weeks post-PBS injection (dog 1, **Figure 1a**), where only stomach Tc-99m uptake was seen as the thyroid and salivary glands were outside the gamma camera field of view. Only faint background blood uptake was present in the heart chambers. There was dose-related myocardial expression as demonstrated by no visible uptake on SPECT imaging with the 5×10^{11} vg dose (dog 2) but incremental uptake with 3×10^{12} vg (dog 3) and 1×10^{13} vg (dog 4) doses at SPECT imaging 2 weeks postinjection (**Figure 1b–d**).

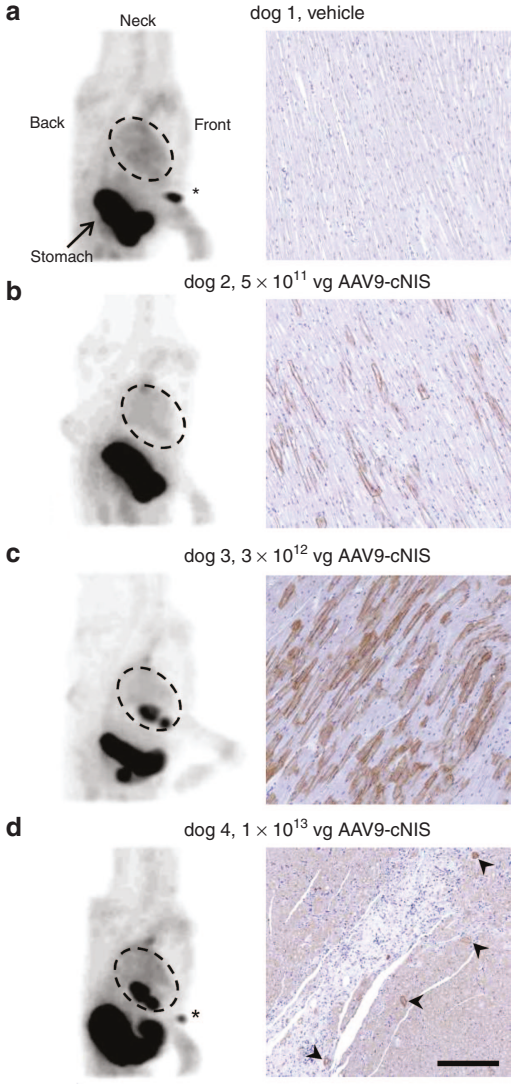

Figure 1 NIS expression following epicardial vector administration. (**a**) Sham dog 1 injected with PBS. (**b–d**) Dogs 2–4 injected with increasing AAV9-cNIS doses. **a–d** Left panels present sagittal maximum intensity projection Tc-99m tomograms imaged 2 weeks after AAV9-cNIS injections. Gamma photon emission is displayed in shades of gray, on a gray scale from no (white) to maximum (black) Tc-99m uptake. Landmarks are noted in dog 1, and hearts are circled in all tomograms. When the Tc-99m injection site at the right forefoot appears it is indicated by an asterix. Right panels are representative immunohistochemistry (IHC) for cNIS (brown staining) in peri-injection LV samples harvested at necropsy after the final imaging. Arrow heads in **d** point at NIS positive cells. Nuclei are counterstained in blue. Bar = 200 µm (applies to all right pictures). AAV, adeno-associated virus; cNIS, canine sodium iodide symporter; IHC, immunohistochemistry.

Further SPECT image analysis was performed to quantify left ventricular (LV) myocardial Tc-99m signal over time using the methodology described in **Figure 2a–f**. Curves integrating the Tc-99m uptake intensity over the LV long axis are presented at all imaging time points for dogs 2–4 with the PBS injected dog as reference (black curve; **Figure 2g**). For dog 2, the LV NIS activity curve was similar to the PBS dog at 2 and 4 weeks. Dog 3 LV NIS activity curves remained stable and above that of the PBS dog out to 10 months. In dog 4, LV NIS activity curves dropped over time and at 6 months postinjection, Tc-99m uptake intensity was similar to the PBS dog curve. Tc-99m uptake was also expressed as the area under the regional LV long axis curves to provide total LV NIS activity at each time point (**Figure 2h**). Global LV expression remained undetectable at 1 month with a dose of 5×10^{11} vg (dog 2), whereas a dose of 3×10^{12} vg yielded stable expression during serial imaging out to 10 months postinjection (dog 3). Finally, the highest LV global expression was observed 2 weeks postinjection with the 1×10^{13} vg dose (dog 4), although expression declined steadily over time and was undetectable by 6 months.

Immunohistochemistry for cNIS was performed using a cNIS rabbit polyclonal antibody on peri-injection site LV samples obtained at necropsy (**Figure 1a–d** right panels). Although cNIS expression was undetectable by SPECT in the dog treated with the 5×10^{11} vg dose, low-level cNIS expression was detectable at the cardiomyocyte membranes (**Figure 1b**). LV samples from the 3×10^{12} dose dog showed higher level of cNIS expression with a mosaic pattern commonly seen on muscle gene delivery[10] (**Figure 1c**), consistent with the NIS activity detected by SPECT imaging. In the dog receiving 1×10^{13} vg there was scant residual cNIS immunostaining (**Figure 1d**, arrows) and monocyte infiltration appeared as clusters of small interstitial cells revealed by their blue nuclei. This suggests there had been a cytotoxic immune response against the transduced cells in the highest dose dog with resulting necrosis and replacement fibrosis (acellular white space).

Intracoronary AAV9-cNIS administration with or without cardiac recirculation

As cardiac gene delivery would be more clinically feasible with intracoronary infusion of vector, the authors studied two dogs with selective intracoronary infusion of 1×10^{13} vg AAV9-cNIS split between the two main (left anterior descending (LAD) and circumflex (Cx)) coronary arteries and administered sequentially ~10 minutes in each coronary.

SPECT imaging detected no cardiac cNIS expression at 2 weeks (**Figure 3a**) and quantitative SPECT analysis demonstrated uptake comparable to the PBS injected dog, 1 and 3 months

© The American Society of Gene & Cell Therapy

postinfusion (dogs 5 and 6, **Figure 3c**). The absence of detectable NIS expression was confirmed by immunostaining LV samples harvested from myocardium supplied by the infused coronary arteries (**Figure 3a**).

As compared to intracoronary infusion, cardiac recirculation has been demonstrated to enhance cardiac expression, therapeutic effects or vg presence for adenovirus, and AAV1 delivered therapeutic genes in an ovine HF model.[3,11] Thus, the authors utilized a percutaneous, anterograde, cardiac-isolated reperfusion circuit to perform cardiac recirculation of AAV9-cNIS for 10 minutes after selective LAD or Cx intracoronary delivery as outlined in **Table 1**. Despite escalating doses (5×10^{12}, 1×10^{13}, and 2×10^{13} vg) of AAV9-cNIS recirculated in a single coronary artery distribution, no cNIS expression was apparent on SPECT imaging at 2 weeks (**Figure 3b**) and quantitative SPECT analysis demonstrated uptake comparable to the PBS injected dog at 2 weeks and 1 month postrecirculation (dogs 7–9, **Figure 3c**). Consistently, no NIS expression was detected by immunohistochemistry (**Figure 3b**).

Quantitative PCR was performed to measure the vector genome copies in LV samples from dogs 5 to 9, as well as in dog 13 where endocardial injections of vector (see in what follows) resulted in areas of the LV that were negative (LV2 and LV3) or positive (LV5 and LV8) by Western blot and immunohistochemistry. qPCR proved more sensitive than immunodetection with

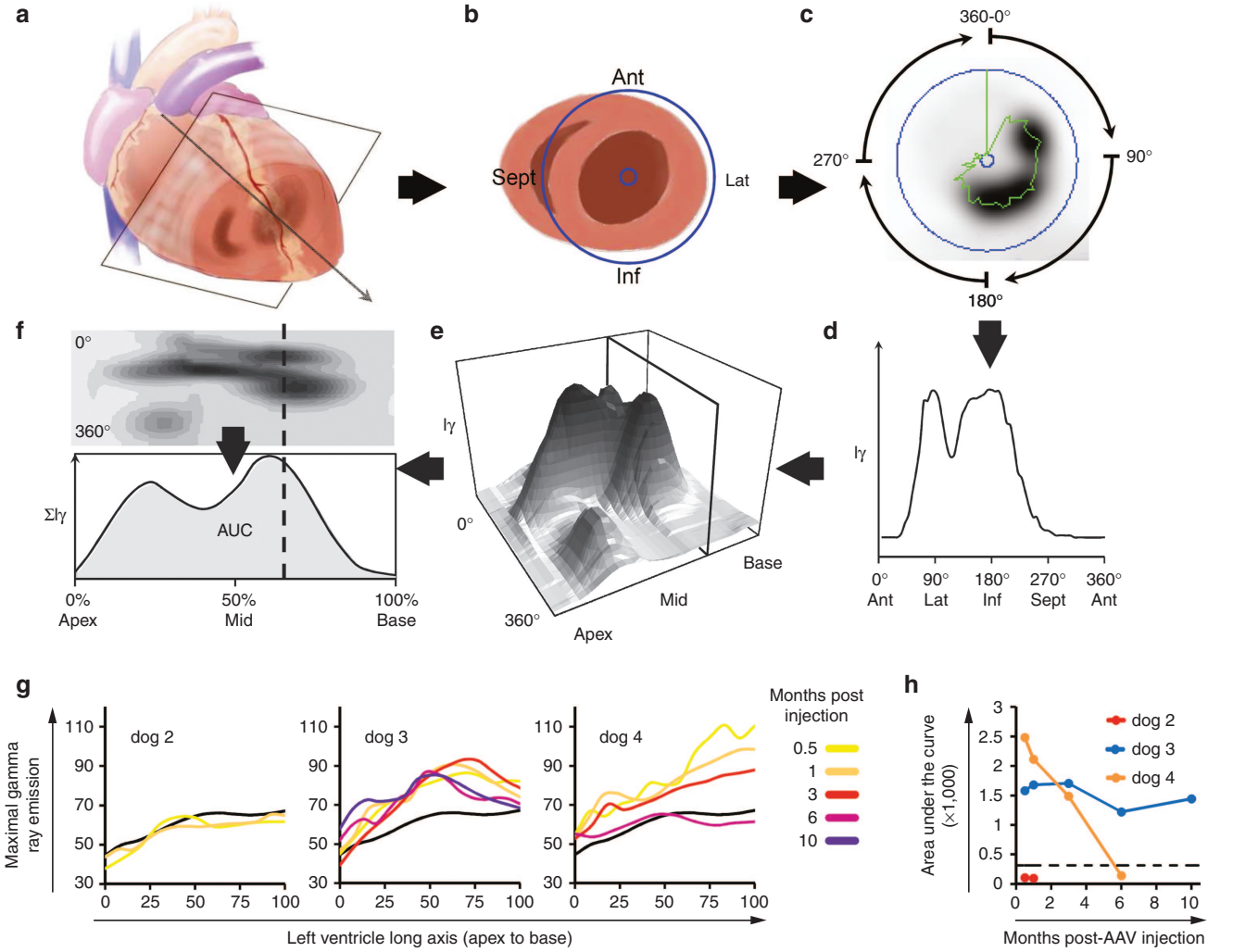

Figure 2 Quantitative SPECT analysis of global left ventricular cNIS transduction over time. (**a**) SPECT myocardial imaging data are reconstructed perpendicular to the left ventricular (LV) long axis to generate short axis (cartoon shown in (**b**)) views of isotope uptake (**c**) with black being most intense uptake. The LV space is defined (purple circles) and maximal gamma ray intensity (Iγ) around the circumference of the short axis is collected every 6° (green trace) and plotted (**d**) for the entire short axis (0–360°). (**e**) The short axis tomogram profiles are compiled from base to apex into a 3D stack plot view or as flat representation in the top (**f**) picture, with Iγ encoded in shades of gray. This enables appreciation of the location and the magnitude of the Tc-99m uptake throughout the whole LV. (**f**) Iγ is integrated for every short axis slice (dashed line) from base to apex to obtain ΣIγ. The area under the ΣIγ curve (AUC; subtracted for background blood uptake) is used as a global LV Tc-99m uptake measure at a specific imaging time. Images and data (**c–f**) shown are from the 3-week imaging in dog 12. (**g**) Quantitative analysis of the LV SPECT imaging from dogs injected endocardially with the C-Cath (ΣIγ curves). The legend on the right defines the correspondence between curve colors and the imaging time postvector injection (in month). Each graph references results from PBS injected dog 1 imaged 2 weeks after the epicardial injection of PBS (black curve). (**h**) Global LV Tc-99m uptake is expressed as the AUC integrating Tc-99m uptake intensity over the long axis of the LV. The AUC obtained for control dog 1 is reported as a dash line threshold for comparison. cNIS, canine sodium iodide symporter; PBS, phosphate buffered saline; SPECT, single-photon emission computerized tomography.

© The American Society of Gene & Cell Therapy

the measurement of 175–1064 copies per μg of DNA in samples LV2 and LV3 from dog 13 that were negative on NIS western blot (**Figure 5b**). Samples from dogs 5 to 9, negative by IHC or imaging, had detectable copy numbers in the same range, whereas results in the NIS positive control samples LV5 and LV8 (see Western blot, **Figure 5b**) were in the range of 10,000–100,000 copies/μg DNA. In theory, transduction in dog 7 should be comparable to dogs 5 and 6 because the dose infused in those latter was split in half and infused down two coronary arteries (see **Table 1**). However, the lower copy number measured in dogs 5 and 7 correlate well with measured levels of pre-existing neutralizing antibodies which may have limited transduction (see **Table 1**). Despite the detection of higher copy number in dogs 8 and 9 that roughly correlate with the twofold vector dose increment, the levels detected in seronegative dogs 6, 8, and 9 were comparable. Yet, dog 6 received half their dose and did not undergo recirculation, suggesting that recirculation did not result in a transduction improvement.

Percutaneous endocardial AAV9-cNIS administration

The robust expression obtained in large animals following intramyocardial injection but not intracoronary infusion of vector is consistent with the classic AAV vector production method from adherent cells. Thus, the authors pursued a clinically feasible percutaneous endocardial injection gene delivery approach.

As compared to standard straight needle endocardial injection, catheters that generate high pressure at the end-hole, a recently described catheter equipped with a curved nitinol alloy needle with side- and end-holes (C-Cath), provides excellent safety, reduced backflow, more uniform injectate distribution, and enhanced myocardial retention of cell therapeutics[12] and was therefore used for the current study. Vector was diluted with PBS and iodinated contrast to allow fluoroscopic confirmation of myocardial injection (see **Supplementary Figure S1b**) and was delivered by 35 injections of 100 μl each. The goal was to position injections circumferentially around the short axis of the LV at three levels from base to apex, avoiding the most distal thin-walled apical segments. One dog was studied using the C-Cath to inject contrast only to establish the technique.

Dose selection for endocardial injection was based on our experience with epicardial injection where 3×10^{11} vg per injection (dog 3) provided robust and durable transgene expression. Three dogs underwent endocardial injections with the same vector dose (~3×10^{11} vg per injection; total dose 1×10^{13} vg) to assess the impact of growing expertise with global endocardial injection (**Table 1**).

SPECT imaging showed robust cardiac cNIS expression at 2 weeks (**Figure 4a**) in all dogs but demonstrated superior distribution of LV expression with growing administration skill. This was because of avoidance of multiple injections in a limited mid-LV

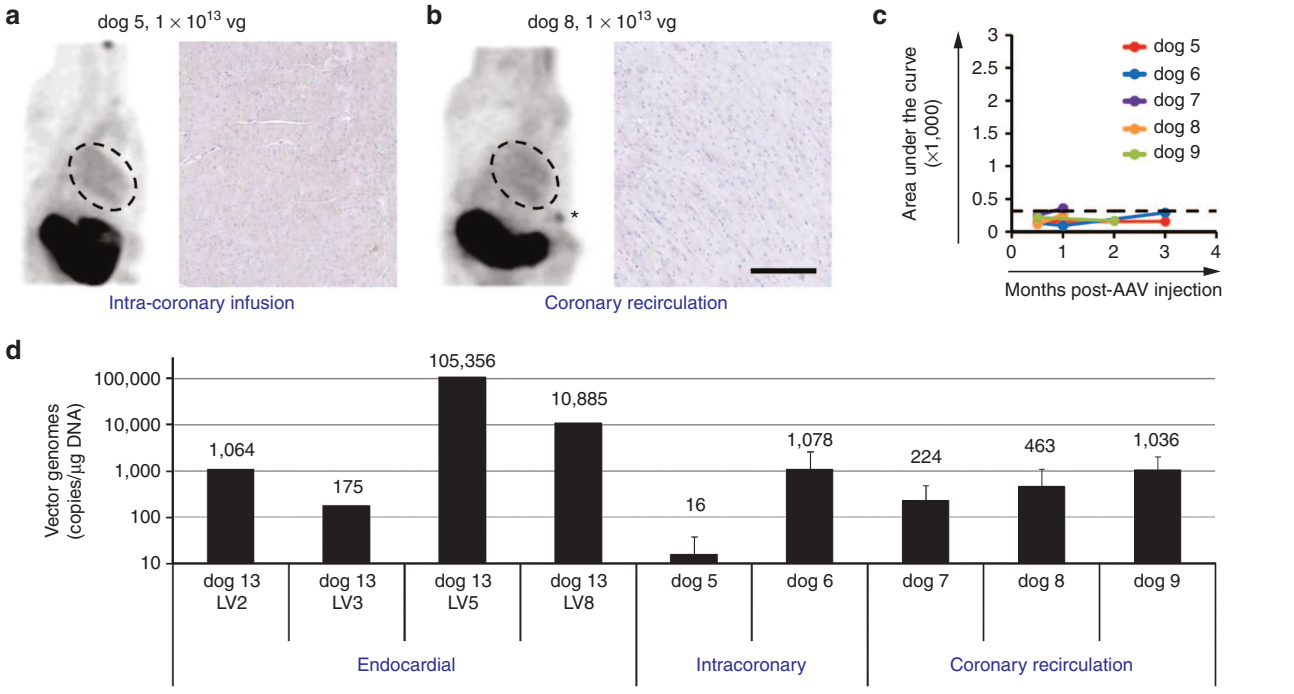

Figure 3 AAV9-NIS transduction following intracoronary vector administration with and without cardiac recirculation. (**a**,**b**) Tc-99m tomograms obtained 2 weeks after vector infusion and cNIS immunostaining on samples harvested at necropsy after final imaging are shown and are representative of findings after intracoronary infusion without and with coronary recirculation. Thyroid is not consistently included in the SPECT window but thyroid uptake is seen in dog 5 (dark spot at top of neck). cNIS immunostainings shown were performed on LV tissue sampled 1 (dog 8) and 3 (dog 5) months postinjection. Bar = 200 μm. (**c**) Global LV Tc-99m uptake is expressed as the area under the curve (AUC) integrating Tc-99m uptake intensity over the long axis of the LV. All dogs that underwent intracoronary infusion without (dogs 5 and 6) or with cardiac recirculation (dogs 7–9) are plotted over imaging time. The black dash line threshold corresponds to PBS dog 1 scintigraphy (see Figure 2a–f for quantification procedure description). (**d**) The vector genome copy number was analyzed by real time PCR in genomic DNA extracted from LV1 and LV2 for dogs 5–9 and results are shown as the average value + SD. Four different LV samples from dog 13 are presented for comparison. AAV, adeno-associated virus; cNIS, canine sodium iodide symporter; PBS, phosphate buffered saline; SPECT, single-photon emission computerized tomography.

© The American Society of Gene & Cell Therapy

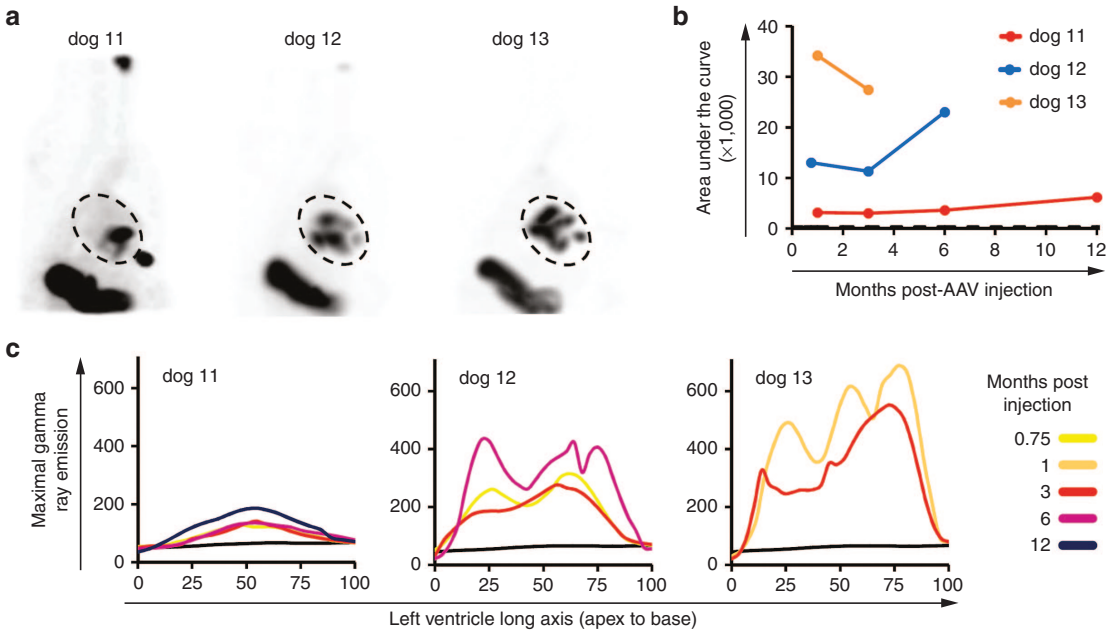

Figure 4 NIS SPECT imaging and quantification following endocardial vector administration. (**a**) Tc-99m tomograms performed 3–4 weeks following the C-Cath endocardial delivery of the vector. (**b**) Global LV Tc-99m uptake is expressed as the area under the integration curves presented in **c.** Control dog 1 threshold is reported as a dash line. (**c**) Quantitative gamma ray emission was plotted against the heart long axis displayed as percentage from apex (0%) to base (100%) as described in Figure 2a–f. A black curve corresponding to the signal of control dog 1 is reported in the three graphs. The color legend on the right defines the imaging times. NIS, sodium iodide symporter; SPECT, single-photon emission computerized tomography.

region as seen with the first attempt (dog 11). In dogs 12 and 13, superior circumferential and longitudinal injection distribution is evident. Signal intensity also increased suggesting superior delivery of vector dose that may be related to more optimal intramural needle positioning with growing experience. Quantitative SPECT analysis demonstrated stable total LV expression over time (up to 12 months; **Figure 4b**) as opposed to epicardial administration of the same total dose but higher injectate per dose in dog 4 (**Table 1**). The quantitative Tc-99m emission curves plotted along the LV long axis illustrate the differences in distribution evident on the tomograms. In dog 11, multiple injections had been performed near one spot in the mid-LV illustrated by the mid-LV peak on the graph (**Figure 4c**). In dogs 12 and 13, the three peaks along the LV long axis quantitative curves graphs reflect more optimal attainment of circumferential injections at the three targeted LV long axis levels.

Assessment of cNIS expression by immunostaining (+ or –) in LV sections with corresponding Western analysis (**Figure 5b**) over a 16 segment LV model (**Figure 5a**) was performed. Consistent with the SPECT imaging, increased total LV expression is seen from dogs 11 to 13. Of note, the septum (LV sections 2, 3, 8, and 9) proved more difficult to target, particularly at the base (LV sections 2 and 3). This is likely because of the small size of the canine LV, hindering the ability to loop the catheter toward the septum. Quantitative analysis of the Western blots show that the maximum expression levels for dogs 11–13 were in the same order of magnitude, as expected because of the same local dose delivery (see **Supplementary Figure S3**).

Immunohistochemistry on full-thickness LV samples allowed assessment of the transmural distribution of cNIS expression (**Figure 5c–f**). Expression was consistently more robust in the midwall and subepicardial regions and relatively scant in the subendocardial regions, potentially owing to the curved needle design. Consistent with SPECT image intensity, higher staining intensities were seen in dogs 12 and 13 as compared to dog 11 or epicardial dog 3 (not shown), despite the injection of similar local vector doses.

Areas with the strongest NIS expression in dogs 12 and 13 consistently displayed monocytic infiltration (**Figure 5f**), whereas dogs 3 and 11 had no inflammation despite receiving the same per injectate dose. The inflammation in dogs 12 and 13 was less intense than was observed with the higher vg per injection epicardial administration (dog 4) and lacked evidence of cellular necrosis or loss of NIS activity on SPECT at 6 months postinjection (dog 12, **Figure 4b**). These data suggest that ~3×10^{11} vg/100 µl injectate constitutes a threshold dose for a noncytotoxic immune response. The inflammatory process may relate to low-level seropositivity detected by the antibody neutralization assay in dogs 12 and 13 but not dogs 3 and 11 (**Table 1**) with reactivation of a memory immune response against the vector capsid but with preservation of transgene expression. However, dog 4 had no evidence of seropositivity on antibody testing (**Table 1**).

Comparison of myocardial injection needle design

A morphometric measure of all transduced areas was performed and established that epicardial injections with a straight needle (dogs 2 and 3) resulted in an average transduction area of $39\pm11\,mm^2$ covering a maximum of ~50% of the LV wall thickness, with the endocardium being negative. The endocardial procedure resulted in a $73\pm45\,mm^2$ average transduction

© The American Society of Gene & Cell Therapy

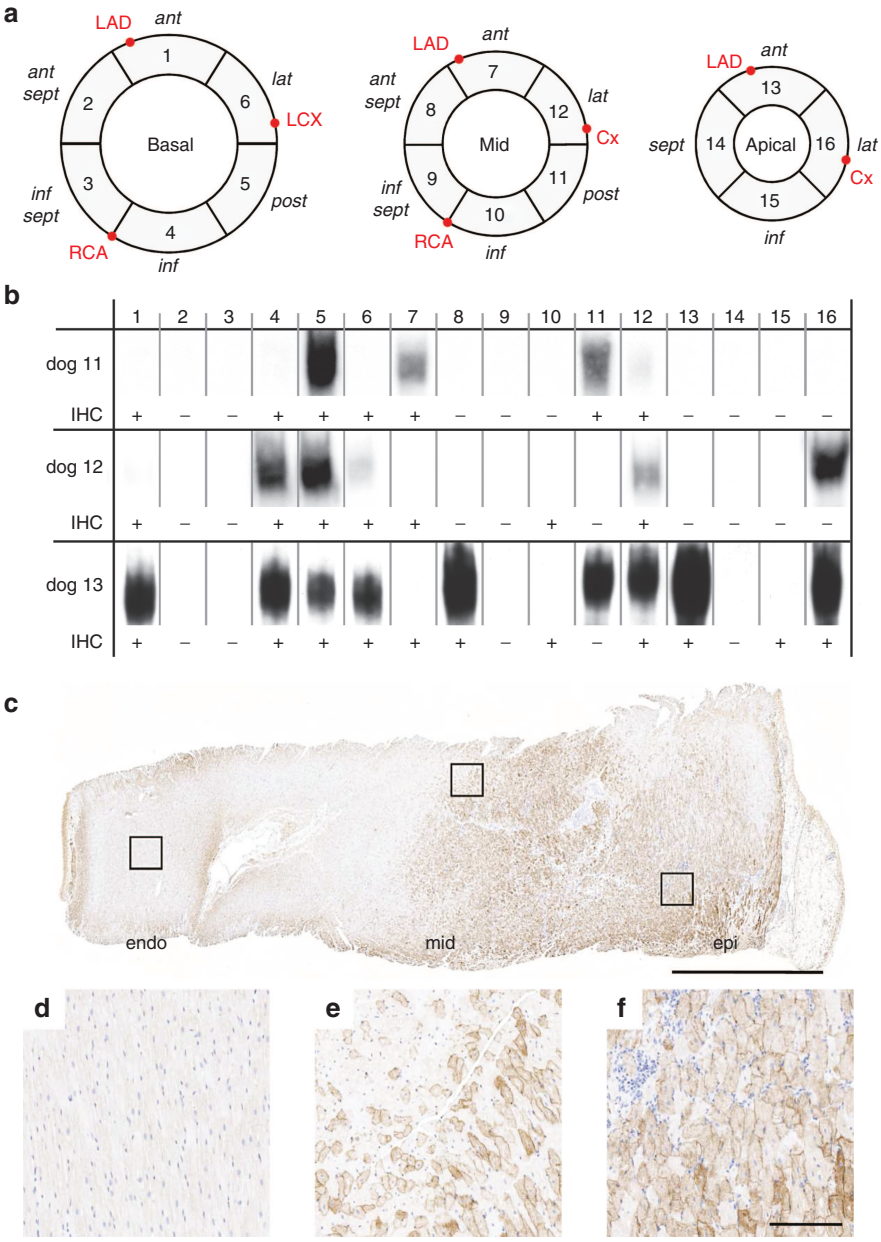

Figure 5 Left ventricular cNIS expression after endocardial injection. (**a**) Diagram of the left ventricular myocardial sampling. Samples are numbered and the positions of each segment analyzed are written in *italic* using the following abbreviations: *ant,* anterior; *lat,* lateral; *post,* posterior; *inf,* inferior; *sept,* septum. The main arteries are also presented in red: LAD, left anterior descending (artery); LCX, left circumflex (coronary artery); Cx, circumflex; RCA, right coronary artery. (**b**) Western blots of cNIS in the 16 LV segments sampled from dogs 11 to 13 administered AAV9-cNIS endocardialy. The bands displayed correspond to the specific semiglycosylated form ~70 KDa (see **Supplementary Figure S2**). Absolute detection of NIS protein by IHC is reported in the corresponding segments below each Western blot (any^{+} or none^{-}). (**c**) Full thickness LV sample from segment 10 of dog 13, which is a representative of NIS positive samples from the endocardial administration group (dogs 11–13). Bar = 3 mm. Panels (**d**–**f**) are respective magnifications of the endocardium, midmyocardium, and subepicardium areas boxed on picture **c**. Bar = 200 µm. AAV, adeno-associated virus; cNIS, canine sodium iodide symporter; IHC, immunohistochemistry.

area, corresponding to 50–100% wall thickness coverage. Under a spherical diffusion model, this translates to 185 versus 472 mm^3, suggesting that the C-Cath curved needle with side holes more than doubled the diffusion volume of the injectates.

DISCUSSION

In this study the authors assessed the effectiveness of several clinically relevant delivery strategies and vector doses for cardiac AAV9 gene transfer in adult immunocompetent dogs using serial SPECT imaging to detect and quantify global cardiac cNIS reporter gene expression over time. Our data establish that direct myocardial injection (epicardial or endocardial) provides far superior gene expression compared to the intracoronary infusion or cardiac recirculation, neither of which provided detectable protein expression at the vector doses tested, although low level vg copy number was detectable by PCR. The authors demonstrate preliminary evidence for a threshold myocardial injection dose that provides robust stable expression for up to 12 months.

© The American Society of Gene & Cell Therapy

To our knowledge, this is the first investigation reporting serial, long-term noninvasive imaging of a transgene delivered to the adult dog heart. Furthermore, the authors provide evidence that the extent of transmural myocardial expression following myocardial vector injection is greater with the C-Cath delivery catheter when compared with an end-hole needle injection system.

Cardiotropism of serotype 9 AAV vectors following IV administration has been extensively demonstrated in rodents.[13–16] However cardiac transduction after IV administration in dogs is lower than would be anticipated from rodent studies.[17] The difference in cardiotropism may reflect the need for dose scale-up when moving from small to large animals as earlier studies have demonstrated higher dose requirements, even in newborn dogs with immature immune systems.[17,18] Alternatively, species tropism differences may exist, as well as vector receptor variation throughout development.

The NIS reporter gene is an active transporter that accumulates radiolabeled substrates and thus concentrates the signal. Therefore the authors postulated that SPECT imaging could be sensitive enough to detect weak NIS activity following the intracoronary infusion of low AAV9 doses in large adult canines. Our data indicate that the intracoronary infusion of up to 2×10^{13} vg results in expression below the sensitivity of our IHC and SPECT detection methodologies. Further, longer intravascular exposure via coronary recirculation for 10 minutes did not enhance NIS expression. A study by Mariani *et al.* using recirculation in a sheep HF model demonstrated that LV levels of ~10,000 vector copies/μg DNA enable the detection of a transgenic protein.[19] The exact threshold needed to provide detectable protein expression is unclear, but our coronary infusion results indicate that levels <1,000 copies per μg DNA are unlikely to achieve noticeable expression by conventional protein detection methodologies. In a recent clinical trial report involving an AAV1 vector and doses similar to ours, Zsebo *et al.* reported levels <500 vector copies per μg DNA several years after coronary infusion.[20] It is possible that vector coronary infusion alone may not be efficient in humans at the dose considered, or that transgene expression decreased over time in pathologic hearts. However, because positive signals of cardiovascular benefit were observed despite low transduction, it would be interesting to determine in a large animal model whether short-term SERCA2a cardiac expression can provide long-lasting benefits. In our case, the time course of intravascular AAV9 clearance (hours) is longer than other serotypes.[15,21] Thus, the 10-minute period of recirculation may be insufficient for AAV9 as opposed to AAV1[3] or the adenoviral vectors whose clearance range is in minutes.[11] The authors speculate that higher AAV9 doses or design of more cardiotropic AAV capsids would be necessary to provide transgene expression in the dog heart after intravascular delivery. Our inability to obtain transgene expression following coronary administration at vector doses comparable to a successful approach in a sheep model[3] may also result from anatomical differences. Indeed, the canine heart has a higher number of collaterals when compared with other large animals which could dilute the infusate and limit expression.

As opposed to intracoronary infusion, direct tissue administration does not require transendothelial vector diffusion into the myocardium. Efficient transduction in that context depends on adequate injection coverage throughout the LV along with optimal diffusion of the injectates. The coverage the authors achieved is comparable to catheter endocardial injections of AAV–green fluorescent protein (GFP) performed in young dogs or adult macaques of 6–10 kg which provided up to 60% GFP positive areas.[8,22] In our hands, septal delivery was more limited than previously reported with other endocardial delivery systems,[8,23] but greater experience, catheter design modifications, or a trans-septal (versus retrograde) approach may enhance septal delivery.

Earlier reports of cardiac radioisotope imaging after NIS gene delivery involved rodents and the use of adenovirus vectors encoding a NIS transgene of human origin.[24–28] In these studies, the adenoviral vector immunogenicity limited the ability to assess long-term (>14 days) expression and therefore did not address the immunogenicity of human NIS protein in immunocompetent rodents. This latter point is of great interest given that the use of the native host's cDNA sequence was demonstrated to be important for long-term expression.[29,30] Our study overexpresses the canine NIS protein in immunocompetent dogs, with long-term expression and activity lasting up to 1 year follow-up. The authors therefore consider the NIS transgene to be relatively nonimmunogenic. That said, an immune response against transgenic NIS protein cannot be ruled out because highly concentrated vector injections resulted in a cytotoxic immune response with gradual loss of the transduced cells at a rate of ~15% per month in dog 4. Earlier studies involving transendocardial delivery of AAV encoding the immunogenic GFP in the young dog or macaques indeed showed some cardiomyocyte degeneration and necrosis as well as mononuclear infiltration at injection sites.[8,22] In contrast the authors obtained long-term expression in four dogs (dogs 3, 11, 12, 13) with ~3×10^{11} vg per injectate, and while two showed local inflammatory infiltrates in areas of high NIS expression, the inflammation was relatively mild compared to that observed with higher injectate dose (dog 4) and neither histology nor serial SPECT imaging revealed signs of cytotoxicity (hematoxylin and eosin (HE) staining histological aspect can be appreciated and compared to NIS staining as shown in **Supplementary Figure S4**). Similarly, an earlier study demonstrated dystrophin expression up to 13 months postendocardial injection using an exon skipping AAV6 vector in a dystrophic dog model.[23] As both dogs demonstrating inflammation had evidence of low level seropositivity on the *in vivo* antibody assay, an immune response against the vector capsid is suggested. Nonetheless, the response was weak compared to an earlier study of AAV vector administration at similar doses to skeletal muscles of seronegative dogs where systematic destruction of the transduced cells independent of the transgene was reported.[31] This observation suggests that the AAV therapeutic to toxic dose window is wider in the heart as compared to skeletal muscles. Although low-level seropositivity may limit expression with intravascular delivery or result in low-level inflammation after myocardial injection at optimal vector doses, our experience with dog 4 (where there was no evidence of seropositivity) suggests that a delayed and cytotoxic immune response can develop in the heart with higher vector doses even in the absence of pre-existing AAV serotype exposure. In perspective, findings would need to be confirmed in different models, and future studies may benefit from alternate imaging modalities with

© The American Society of Gene & Cell Therapy

higher sensitivity such as PET. Future efforts should also evaluate potential metabolic or electrophysiologic effects consequent to the expression of NIS in the heart as its use as a reporter gene should be devoid of adverse effects.

In conclusion, AAV9-based gene delivery has the potential to provide long-term cardiac expression of transgenes using a clinically feasible endocardial delivery strategy. These data are relevant to efforts to translate promising rodent studies of gene therapies to the hearts of larger mammalian species and ultimately, humans with HF.

MATERIALS AND METHODS

Recombinant AAV9 vector production. The AAV vector plasmids pAAV-cNIS and pAAV-hCEA were created by subcloning the canine solute carrier family 5 member 5 cDNA (GenBank XM_541946) synthesized by Genscript (kindly provided by Michael Barry, Mayo Clinic, Rochester, MN) and the human CEA cDNA (GenBankM29540.1) into the pAAV-MCS vector backbone (Stratagene) using EcoRI/XhoI and XbaI/HindIII, respectively. Both transgenes are under the transcriptional control of the cytomegalovirus (CMV) promoter and hGHpolyA sequence.

AAV vectors were generated by packaging AAV2-based recombinant genomes in AAV9 capsids. The production of these pseudotyped AAV2/9 vectors (AAV9) was performed by triple transfection using an adenovirus-free system (Agilent, Santa Clara, CA). In brief, HEK-293T cells were transfected in 15-cm plates using linear polyethylenimine at a N/P ratio of 22 (L-PEI max 25 kDa, Polysciences, Warrington, PA) and a 50-μg equimolar mixture of the three following plasmids per plate: the trans-complementing adenovirus helper plasmid pHelper (Agilent), the pRep2Cap9 packaging plasmid expressing the AAV2 rep gene and the AAV9 cap gene (kindly provided by James M. Wilson, University of Pennsylvania, PA), and a cis-acting AAV vector plasmid (pAAV-cNIS or pAAV-hCEA). After 72 hours of transfection, the collected cells underwent four cycles of freeze/thaw; the crude lysate was then treated with 125 U/ml endonuclease for 1 hour at 37 °C (Benzonase, Merck Millipore, Billerica, MA), then clarified at 13,400 *g* for 20 minutes at 4 °C. The supernatant obtained was resolved by ultracentrifugation at ~400,000 *g* for 2 hours at 4 °C over a discontinuous iodixanol gradient (OptiPrep, Sigma, St. Louis, MO) as described by Lock *et al.*,[32] and iodixanol fractions of density ≥40% were combined, desalted, and concentrated in sterile PBS using centrifugal filter devices (Amicon Ultra-15 MWCO 100K, Millipore). Vector stocks were titrated using real-time quantitative PCR against a standard linear plasmid range by amplifying the human growth hormone polyadenylation signal with forward primer TCT TGG CTC ACT GCA ATC TC, reverse primer GGT CAT GCA TGC CTG GAA TC, and hydrolysis probe TGC CTC AGC CTC CCG AGT TGT TG. All qPCR titers were normalized to a common positive control spiked in every assay and were expressed as encapsidated vgs per milliliter (vg/ml). Average titers of AAV9-cNIS and AAV9-hCEA were 5.18×10^{12} and 9.19×10^{12} vg/ml, respectively.

Neutralization assay. Each dog's serological status to AAV9 capsid was determined with an *in vivo* neutralization assay based on passive immunization of severe combined immunodeficiency mice with candidate dog plasma (200 μl intraperitoneally) 24 hours before IV AAV9-hCEA injection at a dose of 1×10^{11} vg. Background controls (saline intraperitoneally and no AAV9 vector) and maximal expression controls (AAV9-hCEA without plasma) were included. Two weeks post-AAV injection, hCEA expression was assessed by measuring hCEA levels in mouse plasma by ELISA (Elecsys CEA kit, Roche Diagnostics, Indianapolis, IN). The percentage suppression of hCEA expression relative to the maximal expression control with background noise subtraction was calculated. Each assay averaged results from three mice per group.

Animals and vector administrations. This study was approved by the Mayo Institutional Animal Care and Use Committee and conducted in accordance with NIH Guidelines for the Care and Use of Laboratory Animals.

Adult, male, purpose-bred dogs (n = 13; age ~1 year; weight 23.8 ± 3.1 kg) underwent AAV9-cNIS administration via one of the four different administration procedures: direct epicardial injection (via thoracotomy), percutaneous intracoronary infusion, percutaneous intracoronary infusion with cardiac recirculation via a purpose-built coronary sinus catheter, and percutaneous endocardial delivery using a novel endocardial delivery catheter (C-CATHez, Cardio3 Biosciences, Mont St. Guibert, Belgium). Animals were fasted for 14 hours before surgery to prevent morphine-related emetic complications (fasting is also reported to enhance AAV vector transduction following systemic delivery in small animals[33]). Vector doses and imaging follow-up are summarized in **Table 1**. Minor variations in early (2–4 weeks) and intermediate (2–3 months) imaging times were allowed based on scanner access constraints. Decisions to sacrifice at different time points were also influenced by the time needed to develop alternate administration methodologies. The administration protocols are detailed in the following sections and illustrated in **Supplementary Figure S1**.

Epicardial AAV9-cNIS administration. Dogs were premedicated with an intramuscular bolus of 0.5 mg/kg morphine and 0.05 mg/kg atropine. Anesthesia was induced with ketamine 10 mg/kg and diazepam 0.5 mg/kg and maintained on isoflurane (1–2%) and IV antiarrhythmic and analgesic cocktail (3mg/kg/hour lidocaine, 0.6 mg/kg/hour ketamine, and 0.24 mg/kg/hour morphine). A lateral thoracotomy and pericardiotomy was performed. AAV9-cNIS or vehicle (PBS) was then injected via a 31-gage needle into the LV free wall at 10 sites (100 μl each) according to a predefined map (**Supplementary Figure S1**) at three different doses (**Table 1**).

IntracoronaryAAV9-cNIS administration without and with cardiac recirculation. Premedication, anesthesia, and analgesia were as described earlier. Vascular access sheaths (9F, Cordis, Fremont, CA) were placed in the right femoral artery and vein. The right coronary artery is very small and the left main coronary artery is typically very short in the dog. Thus, selective coronary cannulation was performed (5F JL 3.5 LBT, Cordis) with the vector dose split evenly between the LAD and Cx arteries and infused ~10 minutes in each (10 ml total). Although use of nitroglycerin during intracoronary infusion was planned, relative hypotension under anesthesia precluded sustained nitroglycerin infusion.

For animals undergoing cardiac recirculation, a single coronary artery (LAD or Cx) was selectively cannulated for vector infusion. The purpose-designed occlusive balloon catheter was placed in the proximal coronary sinus to allow capture of the coronary venous drainage (V-Focus, Osprey Medical Inc, St Paul, MN). The coronary venous effluent was extracorporally oxygenated and recirculated to the coronary arterial system as described earlier.[11] Once the circuit was established and stable, the vector was delivered in the coronary artery ~10 seconds followed by continued recirculation for a total of 10 minutes. Continuous electrocardiography enabled monitoring for coronary ischemia.

Endocardial AAV9-cNIS administration. Animal premedication, anesthesia, analgesia, and vascular access were as described earlier. Contrast (Omnipaque, GE Healthcare, Little Chalfont, UK) left ventriculograms were performed in the anteroposterior and lateral views and displayed throughout the procedure to provide anatomic landmarks. Endocardial injections were performed using a catheter with a curved delivery needle with side holes (C-Cath).[12] The C-Cath was flushed with heparinized blood before loading with the AAV9-cNIS vector solution mixed with iodine-based contrast (Omnipaque 350 mg I/ml) in 6 : 1 proportion (v/v) to allow visualization of the myocardial injectate (**Supplementary Figure S1b**). The needle length was adjusted based on echocardiographic assessment of LV wall thickness and 35 injections of 100 μl were performed, proceeding circularly from base to apex. Transthoracic echocardiography and fluoroscopy

© The American Society of Gene & Cell Therapy

(in reference to the ventriculogram landmarks) provided the primary guidance for injections as neither intracardiac (8F; AcuNav, Biosense Webster, Diamond Bar, CA) nor transesophageal echo provided incremental information. Transthoracic echocardiography confirmed absence of pericardial effusion during and after theprocedure and beyond transient, self-terminating ventricular ectopic beats, no ventricular arrhythmias were observed. Direct arterial repair was utilized to insure hemostasis after sheath removal.

Animal sacrifice and tissue harvesting. Animals were euthanized (IV sodium pentobarbital) in the week following the last imaging. Myocardium from dogs injected epicardially was sampled near the LV injection points (**Supplementary Figure S1a**). Myocardium from dogs receiving coronary infusion and recirculation hearts were sampled at eight predefined locations (segments 6, 7, 8, 10, 11, 12, 13, and 15, **Figure 5a**). Myocardium from endocardially injected dogs was sampled according to a 16-segment model (**Figure 5a**). Transmural LV sections were fixed in 10% formalin and paraffin embedded or flash frozen in liquid nitrogen and stored at −80 °C.

SPECT/CT imaging. The dogs underwent serial SPECT after AAV9-cNIS as outlined in **Table 1**. Dogs were premedicated (0.5 mg/kg morphine and 0.05 mg/kg atropine intramuscularly) and anesthetized with IV propofol (2–6 mg/kg loading dose titrated to effect followed by 24 mg/kg/hour; APP Pharmaceuticals, Schaumburg, IL) and intubated for airway protection but maintained spontaneous respiration. The electrocardiogram and O_2 saturation were monitored throughout imaging. Tc-99m sodium pertechnetate is well documented to be transported by NIS.[7] Tc-99m was administered intravenously at 0.8 mCi/kg followed by thoracic CT (for anatomical correlation and attenuation correction), followed by a thoracic SPECT image acquisition (20 minutes after Tc-99m). Dogs were placed supine on the SPECT-CT imaging table and imaging was performed using either a GE Hawkeye system (GE Healthcare, Milwaukee, WI) or a Philips Precedence SPECT/CT system (Philips Healthcare, Andover, MA). Both systems were equipped with low-energy high-resolution collimators and were peaked to detect the 140 keV gamma ray emissions from Tc-99m. For SPECT, 60 images were acquired in a 128 × 128 matrix at 30 seconds per image, every 6° or 3° over a 360° rotation on the GE Hawkeye (GE Healthcare, Little Chalfont, UK) system or Philips Precedence system (Philips, Andover, MA), respectively. Transaxial images (3.4 mm thick) were reconstructed using an iterative reconstruction algorithm incorporating attenuation correction (Ordered Subset Expectation Maximization).

Quantitative analysis of cardiac isotope uptake. Quantitation of Tc-99m uptake and thus cNIS expression and activity utilized methodology developed to quantify myocardial perfusion and infarction size in clinical radioisotope cardiac imaging,[34] as illustrated in **Figure 2a–f**. This technique integrates Tc-99m uptake intensity over the long axis of the LV to yield integration curves from which a single value (area under the curve), reflective of global LV transduction, can be extracted.

Blood pertechnetate concentration can vary greatly among different animals or for a single animal over time, for a given radioisotope dose, because of differences in organ uptake and renal clearance disparity. Hence, this inconsistency was corrected by normalizing the gamma-ray emission collected from the LV tissue to the blood activity measured in the same chamber as described by Richard-Fiardo *et al.*[35]

DNA isolation and real-time PCR. LV tissue was homogenized using 2.8-mm ceramic beads on a BeadRuptor apparatus (OMNI International, Kennesaw, GA), followed by genomic DNA isolation with the Wizard Genomic DNA Purification Kit (Promega, Madison, WI) in accordance with the manufacturer's protocol. Total DNA concentration was determined using a Nanodrop ND-1000 spectrophotometer (Thermo Scientific, Wilmington, DE), and 100 ng of DNA of each sample was used as the template material for real-time-PCR. Real-time PCR was performed on each sample by amplifying the CMV promoter to determine copies of the vg. PCR was performed on a 7900 HT thermocycler (Life Technologies, Carlsbad, CA) using Absolute QPCR ROX Mix (Thermo Scientific,), 0.2 µmol/l forward primer CAT CAA TGG GCG TGG ATA GC, 0.2 µmol/l reverse primer GGA GTT GTT ACG ACA TTT TGG AAA, and 0.1 µmol/l hydrolysis probe ATT TCC AAG TCT CCA CCC (5′ FAM and 3′ BHQ1) in a final reaction volume of 18 µl. Cycling conditions consisted of a polymerase activation step at 95 °C for 15 minutes followed by 40 cycles of two steps, 15 seconds of denaturation at 95 °C, and 60 seconds of annealing and extension at 60 °C. A standard dilution range of the linearized AAV vector plasmid containing the CMV sequence was included in each real-time-PCR plate as copy number control. Data is expressed as the number of vg copies per micrograms of genomic DNA.

cNIS western blot analysis. Protein extracts (30 µg per lane) were prepared in sample buffer (12.5% glycerol, 0.1 M Bis–Tris pH7, 1% LDS, 0.5 mmol/l EDTA, and 5 mmol/l tris(2-carboxyethyl)phosphine), resolved by 29 : 1 10% SDS–PAGE and transferred to polyvinylidene fluoride membrane as described earlier.[36] Membranes were blocked in PBS-T including 3% (w/v) BSA for 1 hour at room temperature and incubated overnight at 4 °C with a custom made, affinity purified anti-cNIS rabbit polyclonal antibody. The antibody was prepared by immunizing rabbits by DNA vaccination technology using a sequence encoding amino acids 546–642 of the canine NIS protein (GenBank XP_541946.3), and the collected serum was affinity-purified against the recombinant antigen to obtain the purified polyclonal antibody (Sdix, Newark, DE). Blots were subsequently developed by enhanced chemiluminescent substrate and intensity of the bands was analyzed using ImageLab 5.0 software (Biorad, Hercules, CA). In all cases, a common control sample was loaded in duplicate to allow intensity comparisons across blots. Specificity of our canine NIS antibody was assessed as outlined in **Supplementary Figure S2**.

Immunohistochemistry and histological analysis. Immunostaining of cNIS was performed on 4 µm formalin fixed paraffin embedded (FFPE) sections. Slides were deparaffinized in xylene and tissue was hydrated by a descending ethanol sequence. After rehydration, slides were incubated with H_2O_2 to inactivate endogenous peroxidases and blocked with 10% donkey serum in PBS. The cNIS rabbit polyclonal antibody described earlier was used as primary antibody, and was detected using a horseradish peroxidase conjugated donkey polyclonal secondary antibody to rabbit IgG (Abcam, Cambridge, MA). The immune complex was visualized with diaminobenzidine (Betazoid DAB Chromogen), and nuclei were stained using Tacha's hematoxylin (Biocare Medicals, Concord, CA). After dehydration by an ascending ethanol sequence and cleaning in xylene, slides were mounted using Eukitt (Sigma, St. Louis, MO). Images were obtained with the NDPview2 software and a NanoZoomer slide scanner (Hamamatsu) at a resolution of 0.46 µm/pixel. Morphometric measures of the extent of transmural cNIS expression was performed with the NDPview2 software, for dogs treated with epicardial (straight, end-hole needle) or endocardial (curved needle, side- and end-hole) vector delivery, by tracing circular areas whose diameter encompassed the most distant cNIS positive cells on each section.

HE staining was performed on FFPE sections using Tacha's hematoxylin followed by 1% eosin Y counterstaining (Biocare Medicals), and slides were finally dehydrated and mounted as described earlier.

ACKNOWLEDGMENTS

The authors wish to thank Chad Dewhirst and Broke Gentzler for technical assistance with SPECT imaging. This work was supported by NIH funding RO1 HL105418. The authors have no conflict of interest to disclose.

SUPPLEMENTARY MATERIAL

Figure S1. Intramyocardial injections.
Figure S2. Western-blot validation of the polyclonal cNIS antibody.
Figure S3. Quantification of Western blots from endocardial AAV9-cNIS administrations.
Figure S4. Comparative histological analysis.

© The American Society of Gene & Cell Therapy

REFERENCES

1. Kawase, Y, Ladage, D and Hajjar, RJ (2011). Rescuing the failing heart by targeted gene transfer. *J Am Coll Cardiol* **57**: 1169–1180.
2. Pleger, ST, Shan, C, Ksienzyk, J, Bekeredjian, R, Boekstegers, P, Hinkel, R *et al.* (2011). Cardiac AAV9-S100A1 gene therapy rescues post-ischemic heart failure in a preclinical large animal model. *Sci Transl Med* **3**: 92ra64.
3. Byrne, MJ, Power, JM, Preovolos, A, Mariani, JA, Hajjar, RJ and Kaye, DM (2008). Recirculating cardiac delivery of AAV2/1SERCA2a improves myocardial function in an experimental model of heart failure in large animals. *Gene Ther* **15**: 1550–1557.
4. Pepe, M, Mamdani, M, Zentilin, L, Csiszar, A, Qanud, K, Zacchigna, S *et al.* (2010). Intramyocardial VEGF-B167 gene delivery delays the progression towards congestive failure in dogs with pacing-induced dilated cardiomyopathy. *Circ Res* **106**: 1893–1903.
5. Jessup, M, Greenberg, B, Mancini, D, Cappola, T, Pauly, DF, Jaski, B *et al.*; Calcium Upregulation by Percutaneous Administration of Gene Therapy in Cardiac Disease (CUPID) Investigators. (2011). Calcium Upregulation by Percutaneous Administration of Gene Therapy in Cardiac Disease (CUPID): a phase 2 trial of intracoronary gene therapy of sarcoplasmic reticulum Ca2+-ATPase in patients with advanced heart failure. *Circulation* **124**: 304–313.
6. Hingorani, M, Spitzweg, C, Vassaux, G, Newbold, K, Melcher, A, Pandha, H *et al.* (2010). The biology of the sodium iodide symporter and its potential for targeted gene delivery. *Curr Cancer Drug Targets* **10**: 242–267.
7. Zuckier, LS, Dohan, O, Li, Y, Chang, CJ, Carrasco, N, Dadachova, E *et al.* (2004). Kinetics of perrhenate uptake and comparative biodistribution of perrhenate, pertechnetate, and iodide by NaI symporter-expressing tissues in vivo. *J Nucl Med* **45**: 500–507.
8. Bish, LT, Sleeper, MM, Brainard, B, Cole, S, Russell, N, Withnall, E *et al.* (2008). Percutaneous transendocardial delivery of self-complementary adeno-associated virus 6 achieves global cardiac gene transfer in canines. *Mol Ther* **16**: 1953–1959.
9. Penheiter, AR, Russell, SJ and Carlson, SK (2012). The sodium iodide symporter (NIS) as an imaging reporter for gene, viral, and cell-based therapies. *Curr Gene Ther* **12**: 33–47.
10. Blankinship, MJ, Gregorevic, P, Allen, JM, Harper, SQ, Harper, H, Halbert, CL *et al.* (2004). Efficient transduction of skeletal muscle using vectors based on adeno-associated virus serotype 6. *Mol Ther* **10**: 671–678.
11. Kaye, DM, Preovolos, A, Marshall, T, Byrne, M, Hoshijima, M, Hajjar, R *et al.* (2007). Percutaneous cardiac recirculation-mediated gene transfer of an inhibitory phospholamban peptide reverses advanced heart failure in large animals. *J Am Coll Cardiol* **50**: 253–260.
12. Behfar, A, Latere, JP, Bartunek, J, Homsy, C, Daro, D, Crespo-Diaz, RJ *et al.* (2013). Optimized delivery system achieves enhanced endomyocardial stem cell retention. *Circ Cardiovasc Interv* **6**: 710–718.
13. Pacak, CA, Mah, CS, Thattaliyath, BD, Conlon, TJ, Lewis, MA, Cloutier, DE *et al.* (2006). Recombinant adeno-associated virus serotype 9 leads to preferential cardiac transduction in vivo. *Circ Res* **99**: e3–e9.
14. Vandendriessche, T, Thorrez, L, Acosta-Sanchez, A, Petrus, I, Wang, L, Ma, L *et al.* (2007). Efficacy and safety of adeno-associated viral vectors based on serotype 8 and 9 vs. lentiviral vectors for hemophilia B gene therapy. *J Thromb Haemost* **5**: 16–24.
15. Zincarelli, C, Soltys, S, Rengo, G and Rabinowitz, JE (2008). Analysis of AAV serotypes 1-9 mediated gene expression and tropism in mice after systemic injection. *Mol Ther* **16**: 1073–1080.
16. Inagaki, K, Fuess, S, Storm, TA, Gibson, GA, Mctiernan, CF, Kay, MA *et al.* (2006). Robust systemic transduction with AAV9 vectors in mice: efficient global cardiac gene transfer superior to that of AAV8. *Mol Ther* **14**: 45–53.
17. Yue, Y, Ghosh, A, Long, C, Bostick, B, Smith, BF, Korneygay, JN *et al.* (2008). A single intravenous injection of adeno-associated virus serotype-9 leads to whole body skeletal muscle transduction in dogs. *Mol Ther* **16**: 1944–1952.
18. Pan, X, Yue, Y, Zhang, K, Lostal, W, Shin, JH and Duan, D (2013). Long-term robust myocardial transduction of the dog heart from a peripheral vein by adeno-associated virus serotype-8. *Hum Gene Ther* **24**: 584–594.
19. Mariani, JA, Smolic, A, Preovolos, A, Byrne, MJ, Power, JM and Kaye, DM (2011). Augmentation of left ventricular mechanics by recirculation-mediated AAV2/1-SERCA2a gene delivery in experimental heart failure. *Eur J Heart Fail* **13**: 247–253.
20. Zsebo, K, Yaroshinsky, A, Rudy, JJ, Wagner, K, Greenberg, B, Jessup, M *et al.* (2014). Long-term effects of AAV1/SERCA2a gene transfer in patients with severe heart failure: analysis of recurrent cardiovascular events and mortality. *Circ Res* **114**: 101–108.
21. Kotchey, NM, Adachi, K, Zahid, M, Inagaki, K, Charan, R, Parker, RS *et al.* (2011). A potential role of distinctively delayed blood clearance of recombinant adeno-associated virus serotype 9 in robust cardiac transduction. *Mol Ther* **19**: 1079–1089.
22. Gao, G, Bish, LT, Sleeper, MM, Mu, X, Sun, L, Lou, Y *et al.* (2011). Transendocardial delivery of AAV6 results in highly efficient and global cardiac gene transfer in rhesus macaques. *Hum Gene Ther* **22**: 979–984.
23. Bish, LT, Sleeper, MM, Forbes, SC, Wang, B, Reynolds, C, Singletary, GE *et al.* (2012). Long-term restoration of cardiac dystrophin expression in golden retriever muscular dystrophy following rAAV6-mediated exon skipping. *Mol Ther* **20**: 580–589.
24. Miyagawa, M, Beyer, M, Wagner, B, Anton, M, Spitzweg, C, Gansbacher, B *et al.* (2005). Cardiac reporter gene imaging using the human sodium/iodide symporter gene. *Cardiovas Res* **65**: 195–202.
25. Miyagawa, M, Anton, M, Wagner, B, Haubner, R, Souvatzoglou, M, Gansbacher, B *et al.* (2005). Non-invasive imaging of cardiac transgene expression with PET: comparison of the human sodium/iodide symporter gene and HSV1-tk as the reporter gene. *Eur J Nucl Med Mol Imaging* **32**: 1108–1114.
26. Rao, VP, Miyagi, N, Ricci, D, Carlson, SK, Morrus, JC, Federspiel, MJ *et al.* (2008). Sodium iodide symporter (hNIS) permits molecular imaging of gene transduction in cardiac transplantation. *Transplantation* **84**: 1662–1666.
27. Lee, K, Kim, HK, Paik, JY, Matsui, T, Choe, YS, Choi, Y *et al.* (2005). Accuracy of myocardial sodium/iodide symporter gene expression imaging with radioiodide: evaluation with a dual-gene adenovirus vector. *J Nucl Med* **46**: 652–657.
28. Ricci, D, Mennander, AA, Pham, LD, Rao, VP, Miyagi, N, Byrne, GW *et al.* (2008). Non-invasive radioiodine imaging for accurate quantitation of NIS reporter gene expression in transplanted hearts. *Eur J Cardiothorac Surg* **33**: 32–39.
29. Tripathy, SK, Black, HB, Goldwasser, E and Leiden, JM (1996). Immune responses to transgene-encoded proteins limit the stability of gene expression after injection of replication-defective adenovirus vectors. *Nat Med* **2**: 545–550.
30. Moulay, G, Masurier, C, Bigey, P, Scherman, D and Kichler, A (2010). Soluble TNF-α receptor secretion from healthy or dystrophic mice after AAV6-mediated muscle gene transfer. *Gene Ther* **17**: 1400–1410.
31. Wang, Z, Allen, JM, Riddell, SR, Gregorevic, P, Storb, R, Tapscott, SJ *et al.* (2007). Immunity to adeno-associated virus-mediated gene transfer in a random-bred canine model of Duchenne muscular dystrophy. *Hum Gene Ther* **18**: 18–26.
32. Lock, M, Alvira, M, Vandenberghe, LH, Samanta, A, Toelen, J, Debyser, Z *et al.* (2010). Rapid, simple, and versatile manufacturing of recombinant adeno-associated viral vectors at scale. *Hum Gene Ther* **21**: 1259–1271.
33. Moulay, G, Scherman, D and Kichler, A (2010). Fasting increases the *in vivo* gene delivery of AAV vectors. *Clin Transl Sci* **3**: 333–336.
34. Gibbons, RJ, Verani, MS, Behrenbeck, T, Pellikka, PA, O'Connor, MK, Mahmarian, JJ *et al.* (1989). Feasibility of tomographic 99mTc-hexakis-2-methoxy-2-methylpropyl-isonitrile imaging for the assessment of myocardial area at risk and the effect of treatment in acute myocardial infarction. *Circulation* **80**: 1277–1286.
35. Richard-Fiardo, P, Franken, PR, Lamit, A, Marsault, R, Guglielmi, J, Cambien, B *et al.* (2012). Normalisation to blood activity is required for the accurate quantification of Na/I symporter ectopic expression by SPECT/CT in individual subjects. *PLoS One* **7**: e34086.
36. Han, YS and Ogut, O (2011). Force relaxation and thin filament protein phosphorylation during acute myocardial ischemia. *Cytoskeleton (Hoboken)* **68**: 18–31.